Debris Albedo from Laser Ablation in Low and High Vacuum: Comparisons to Hypervelocity Impact

Gouri Radhakrishnan, Paul M. Adams, Diana R. Alaan, Christopher J. Panetta
Space Materials Laboratory, The Aerospace Corporation
Mail Station M2-248, 2310 E. El Segundo Blvd., El Segundo, CA 90245

ABSTRACT

The albedo of orbital debris fragments in space is a critical parameter used in the derivation of their physical sizes from optical measurements. The change in albedo results from scattering due to micron and sub-micron particles on the surface. There are however no known hypervelocity collision ground tests that simulate the high-vacuum conditions on-orbit. While hypervelocity impact experiments at a gun range can offer a realistic representation of the energy of impact and fragmentation, and can aid the understanding of albedo, they are conducted in low-pressure air that is not representative of the very high vacuum of 10^{-8} Torr or less that exists in the Low Earth Orbit environment. Laboratory simulation using laser ablation with a high power laser, on the same target materials as used in current satellite structures, is appealing because it allows for well-controlled investigations that can be coupled to optical albedo (reflectance) measurements of the resultant debris. This relatively low-cost laboratory approach can complement the significantly more elaborate and expensive field-testing of single-shot hypervelocity impact on representative satellite structures. Debris generated is optically characterized with UV-VIS-NIR reflectance, and particle size distributions can be measured. In-situ spectroscopic diagnostics (nanosecond time frame) provide an identification of atoms and ions in the plume, and plasma temperatures, allowing a correlation of the energetics of the ablated plume with resulting albedo and particle size distributions of ablated debris. Our laboratory experiments offer both a high-vacuum environment, and selection of any gaseous ambient, at any controlled pressure, thus allowing for comparison to the hypervelocity impact experiments in low-pressure air. Initial results from plume analysis, and size distribution and microstructure of debris collected on witness plates show that laser ablations in low-pressure air offer many similarities to the recent DebrisLV and DebriSat hypervelocity impact experiments, while ablations in high-vacuum provide critical distinctions.

1. INTRODUCTION

The major concern with debris is that it might hit an operational spacecraft or a larger manned object such as the ISS with detrimental consequences. Hence there is a basic need to gather orbital object data to accurately define a space environment, and tremendous interest in determining debris object sizes [1-10], for which albedo of debris surfaces is critical.

Understanding space debris relies heavily on an understanding of hypervelocity impact (HVI), which in turn plays a crucial role in current fragmentation modelling predictions. Low earth orbit (LEO) and geosynchronous orbit (GEO) are the most crowded orbits and numerous radar and optical measurements are being conducted to identify the material composition of space debris, as well as, establish their physical sizes [1-9]. A critical parameter for the interpretation of physical sizes of the space debris particles from optical measurements is the albedo of fragments [4-6]. Currently observations of debris in LEO are conducted with radar [1-3], while optical observations are mostly used for observation of debris in GEO [7-10]. In 2007, ESCG and NASA JSC recommended the use of a global albedo value of 0.13 for debris objects [4], then revised this to 0.175 [5]. As called out by the authors, additional calculations from alternate photometric data and research are needed for establishing more accurate albedo values (for more accurate size estimation).

While hypervelocity impact experiments at a gun range can offer a realistic representation of the energy of impact and fragmentation, they are not typically performed at extremely low pressures of 10^{-8} Torr or lower, that are representative of the low-earth orbit (LEO) environment. According to Pirri [11], the use of laser ablation to simulate hypervelocity shock in a material could be accomplished by setting the laser spot equal to the diameter of the particles and the pulse duration equal to the particle impact duration. Arad [12] looked at the similarity between

impact events in space and laser impacts by comparing crater morphology in aluminium, gold and alumina, and by discharge initiation on metal-oxide-silicon capacitor impact detectors. Tandy et al. [13] used a 2-stage light gas gun to accelerate 5 mg nylon cylinders to speeds of 5 -7 km/s. They used UV-visible emission spectroscopy and high-speed imaging to study the process. Heunoske et al. [14] investigated impact experiments on solar panels using a two-stage light gas gun to accelerate aluminum spheres of a few mm and measured plasma properties.

Laser ablation differs from hypervelocity impact in that the laser material interaction occurs at the surface, leading to rapid heating and vaporization of the surface layer. This then results in a high pressure that creates a shock in the target. In hypervelocity impact, the projectile goes right through the bulk of the target. We have calculated the energy/unit mass of Al in the hypervelocity impact vs. laser ablation experiments. For the DebriSat test, the mass of the Al projectile was 580 g, and its velocity was 6800 m/s. This corresponds to a kinetic energy (KE) of 1.32×10^7 J. Upon hitting the first surface, which was Al honeycomb (mass 8.9 g, velocity 0 km/s), the velocity of the projectile gets reduced to 6700 m/s and the corresponding KE was 1.28×10^7 J. The difference in KE was 4×10^5 J. This is the KE that was dispersed in 8.9 g of Al honeycomb. Hence the energy from the hypervelocity impact per unit mass of Al honeycomb was 4.5×10^4 J/g. In the case of laser ablation, for a fluence of 10 J/cm^2, when absorbed within 100 nm of Al target, the corresponding volume is 10^{-5} cm^3. The mass of Al hit by the laser is this volume times its density (2.7 g/cm^3). Hence the laser energy per unit mass of Al is 10 J/2.7×10^{-5} g, or 3.5×10^5 J/g. This is within a factor of 10 of the hypervelocity impact on the first surface, and is easily the same, if the absorption depth ranges from 100 nm to 1000 nm.

We demonstrated our ability to duplicate DebriSat hypervelocity gun-range test data in air using the laser ablation technique and used this as a baseline for recreating the deposition process that occurs during hypervelocity collisions in high-vacuum [15]. The experiments could be conducted in high-vacuum (10^{-7}-10^{-8} Torr) and offered the flexibility of selecting any gaseous ambient, at any controlled pressure, thus allowing for comparison to the hypervelocity impact experiments in low-pressure air. The setup is also appealing because it provides the opportunity to investigate the effects of various parameters in a well-controlled and repeatable environment. Another important attribute of conducting laboratory measurements is that it does not require foam catch panels (used in DebrisLV and DebriSat experiments [16,17] to catch fragments) that interfered with microscopic debris analyses and albedo measurements. Experiments are coupled with optical characterizations (UV-VIS-NIR reflectance), chemical characterization, surface morphology, and particle size distributions of the debris. In-situ spectroscopic identification of atoms and ions in the plume as a function of incident laser fluence is used to correlate energetics of the ablated plume with resulting particle size distributions of ablated debris and corresponding albedo. Initial results from spectroscopic plume analysis, and the microstructure and size distributions of ablated debris collected on witness plates show that laser ablations in low-pressure air offer many similarities to the hypervelocity impact experiments, while ablations in high-vacuum provide critical distinctions.

Specifically, we have tried to understand and compare the microstructure and albedo of debris generated by laser ablation to the hypervelocity impacts on DebrisLV and DebriSat, conducted jointly by the Space and Missile Systems Center (SMC), National Aeronautics and Space Administration (NASA), The Aerospace Corporation, Arnold Engineering Development Center (AEDC), and University of Florida. The test (conducted on April 15, 2014) was aimed at simulating an on-orbit destructive collision of a modern satellite by a hypervelocity projectile. Additional details and the results of spectroscopic measurements on the flash from the hypervelocity impact on DebriSat have been previously described [16]. In the DebriSat hypervelocity impact test, the projectile was a hollow Al cylinder, and the target was a simulated satellite structure with an exterior honeycomb 6061 Al structure having a carbon composite face sheet and the interior filled with various components representative of a real satellite. Time-resolved spectra from 0 to 1 millisecond were measured in microsecond increments using a similar set up as described later. These spectra were collected using a low-resolution 150 groove/mm grating in order to capture the largest possible spectral bandwidth in this one-shot experiment. In addition, witness plates were positioned along the walls of the vacuum chamber enclosing the satellite structures to collect debris produced by the impact. The plates contained aluminum stubs for the scanning electron microscope, as well as coupons of Si, Ge, and fused silica. Reflectance from the coupons had been measured prior to the test to establish a reference. Optical reflectance of debris-coated coupons was measured after the test.

In our recent work [15] we showed that the albedo of debris fragments is dependent on the optical properties of surface coatings comprising nano-micro particulates generated by impact. The resulting surface morphology greatly influences the scatter and hence the reflectance. We have also shown that debris due to Al oxide has a vastly different optical reflectance than from Al. Hence we have taken the approach to make experimental measurements of albedo from debris surfaces produced by laser-induced impact in high-vacuum, to replicate hypervelocity impact in LEO.

2. EXPERIMENTAL DETAILS

This work was focused on ablating Al 6061 alloy as this is the primary material used in the DebriSat and Debris LV structures. Laser ablations were conducted in vacuum and in air with a high-power excimer laser (Lambda-Physik LPX 210i). The target, a 25-mm diameter disc of Al 6061, was held in a stainless steel vacuum chamber at a 45-deg angle to the incoming laser beam. In addition, we designed a target that comprised equal volumes of Al 6061 with a PAN-based carbon-fiber reinforced composite to simulate the role of a composite facesheet on Al honeycomb in a satellite structure. The chamber is pumped by a turbomolecular pump to a maximum base pressure of 10^{-8} Torr, and has gas inlets for various gases. Laser ablations of the 6061 Al target were conducted both in 2 Torr air, as well as in high vacuum (10^{-7} Torr), while the Al-composite target was only ablated in high vacuum.

The experimental setup is shown in Fig. 1. Deposited materials were collected on single-crystal silicon and copper substrates held at a distance of ~ 50 mm in front of, and parallel to, the target. Spectroscopic identification of atoms and ions in the ablation plume was conducted as a function of laser fluence. These measurements were made by imaging the plume through a fused silica port via a 3-m long optical fiber to a gated ICCD camera, (PIMAX3) coupled to a spectrometer (320 PI). Following a TTL trigger input from the excimer laser supplied to the CCD camera, the CCD was gated with allowed gate widths ranging from 4 nanoseconds (ns) to 1 millisecond (ms). The spectrometer is equipped with 3 gratings: 150 grooves/mm and 600 grooves/mm, both blazed at 300 nm, and a holographic 2400 groove/mm grating blazed in the UV.

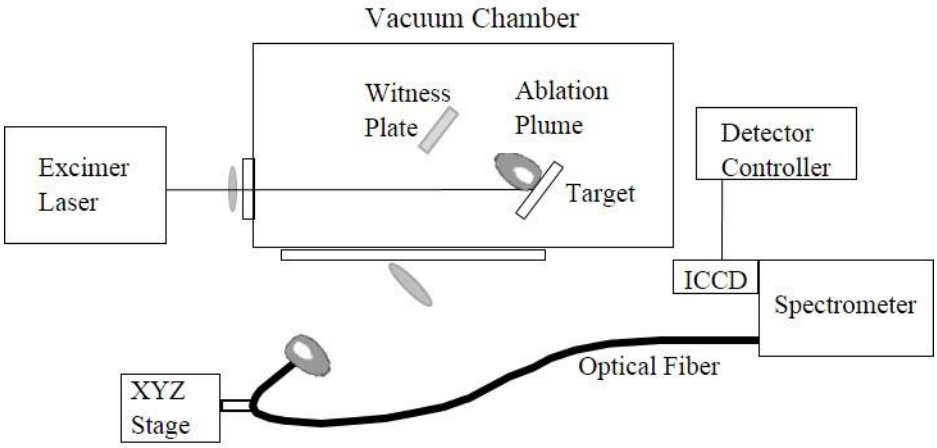

Fig. 1 Schematic of experimental setup for laser ablation

Deposited materials were examined in a JEOL 7600F field emission scanning electron microscope (FE-SEM) at 2KV, 5KV and 15KV in order to tailor the penetration depth. Silicon samples were cleaved and the edges were examined to determine the thickness of deposits. Energy dispersive spectroscopy (EDS) was performed with an Oxford Instruments X-Max silicon drift detector (SSD) at 5KV and 20KV in order to control the penetration depth. Approximately 0.15 mm^2 areas were scanned to determine the extent of aluminum coverage on silicon samples. Particle size measurements were made from the SEM images (1KX) using Image-J software from the National Institutes of Health.

Pre-and post-deposition optical characterizations (UV-VIS-NIR reflectance) on Cu /Si substrates were conducted to understand debris darkening as a function of impact conditions. Specular reflection measurements were made on a Perkin Elmer Lambda 950 spectrophotometer equipped with a Universal Reflectance Accessory (URA). The URA performs a V-N type absolute specular reflection measurement where the only difference between the reference configuration and sample configuration is the reflection off the sample. Measurements were made with depolarized light at an 8-deg angle of incidence, with a spot size of 3.5mm x 4mm on the sample. The field of view of the detector is extremely narrow and aligned with the specular beam, therefore any scattered light appreciably off specular will not make it to the detector and will register as a "loss" in reflection in the resulting data.

Total hemispherical reflection measurements were made with a Perkin Elmer Lambda 900 spectrophotometer

equipped with a Labsphere PELA 1000 integrating sphere attachment. The PELA 1000 can also measure selectively the diffuse component of reflection by allowing the specular beam to exit the sphere (and, therefore, not be collected by the detector). From this, specular reflectance can be calculated by subtracting the diffuse component of the reflectance from the total hemispherical reflectance. For this work, reflection measurements were made at an 8-deg angle of incidence, relative to a Spectralon reference material. An NBS 2019d white tile was also measured in the same configuration, to make the relative measurements absolute. This was accomplished by comparing the relative reflection measurement of the tile with the certified values and applying correction factors to ensure the two spectra overlay. These factors would then commute to the scans of the samples.

3. RESULTS AND DISCUSSION

Ablation of a 6061 Al target was conducted in air (ranging from 0.5 Torr to 2 Torr). When the collected debris was imaged in the SEM at 2 KV at high magnifications (Fig. 2a), fine filamentous structures similar to Debris-LV/DebriSat (Fig. 2b) are seen from laser-ablated material.

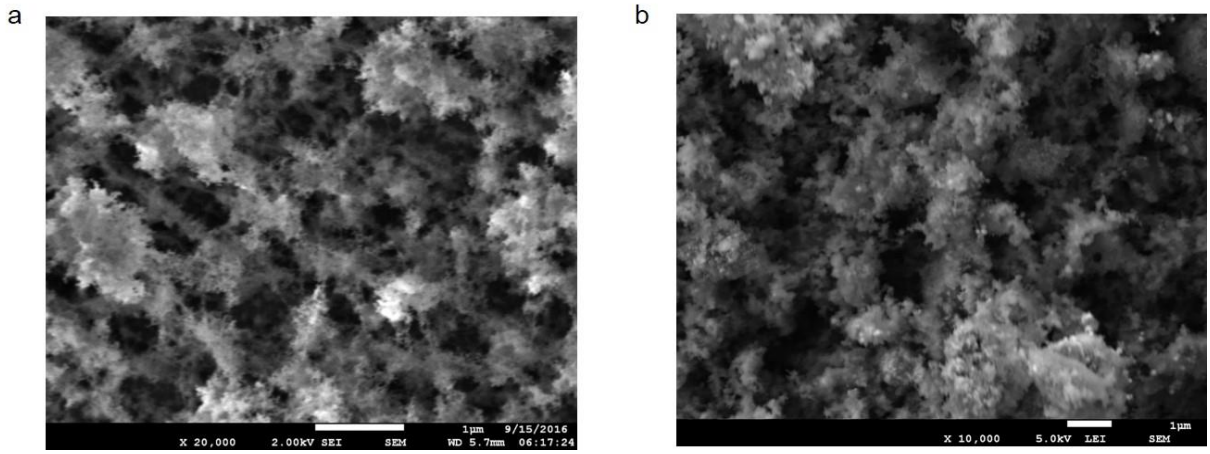

Fig. 2. Debris collected from 6061 Al target (a) laser ablation in 2 Torr air (b) hypervelocity impact on DebriSat in 2 Torr air

The key observed difference between laser ablation in air and in high-vacuum (Fig. 3) is that in air, filaments of aluminum oxide (Al_xO_y) are produced with embedded spherical particles of Al that are covered by the oxide (Fig. 3b), as observed in lower magnification SEM images (EDS data not shown here), but in high-vacuum, a metallic film of Al is produced and flattened Al particles (splats) are deposited over this Al film (Fig. 3a). In addition to filaments of Al_xO_y, laser ablation in air at low fluences (6-10 J/cm^2) (Fig. 3b) produces small, spherical particles, which closely match those observed in hypervelocity impact debris measured with Debris-LV.

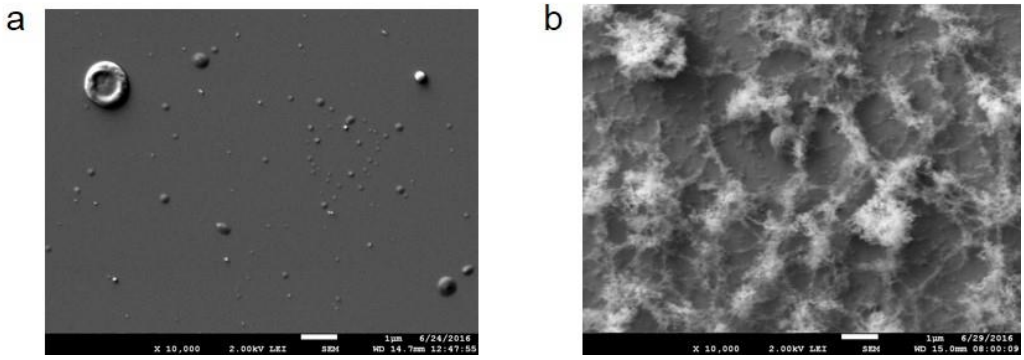

Fig. 3. Debris from laser ablation at 7 J/cm^2 (a) in high-vacuum, (b) in air. Images are at 10 KX and were taken at 2 KV

In high-vacuum the ablated material in the gas phase and liquid droplets travel to the substrate without collisions. The liquid droplets flatten upon impacting the substrate, and are observed as splats. In air, collisional cooling of the ablated plume by background gas molecules results in solidification of the ejected liquid droplets, in-flight, as they travel to the substrate, evidenced by perfectly spherical particles that are a core of Al metal covered by a sheath of oxide, as opposed to splats of Al metal. In addition fine filaments (of Al_xO_y) are produced on the witness plate and it is likely that these are produced from gas-phase reactions between ablated Al and air molecules.

Particle size distributions are shown in Fig. 4 for high and low fluence ablations in high-vacuum, as well as that measured with DebrisLV. For DebrisLV and laser ablation air samples, 15 KV SEM images were needed to reveal particles buried in Al oxide filaments.

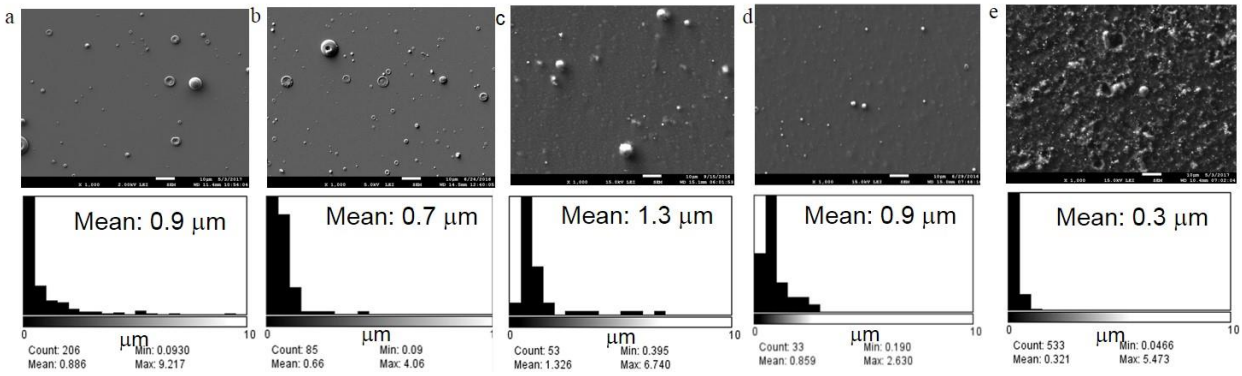

Fig. 4. SEM images (1KX) and particle size distributions: laser ablation in high-vacuum (a) 19 J/cm^2; (b) 10 J/cm^2; laser ablation in air (c) 19 J/cm^2; (d) 10 J/cm^2; (e) HVI, air, DebrisLV. Laser ablation in air samples were imaged at 15 KV in order make the spherical Al droplets visible through the Al_xO_y filaments.

Table 1 summarizes the distributions for all conditions. Measurements for DebriSat were impeded by intense soft catch covering the debris.

Table 1: Measured Particle Size Distributions

Laser Ablation High-vacuum/High Fluence	Laser Ablation High-vacuum/Low Fluence	Laser Ablation Air/High Fluence	Laser Ablation Air/Low Fluence	DebriSat/Air	DebrisLV/Air
Mean 0.9 μm Mode 0- 0.5 μm	Mean 0.7 μm Mode 0-0.5 μm	Mean 1.3 μm Mode 0.5-1.0 μm	Mean 0.9 μm Mode 0.5-1.0 μm	No measurements due to intense soft catch	Mean 0.3 μm Mode 0-0.5 μm

Laser ablation of a 6061 Al target at a vacuum of 10^{-7} to 10^{-8} Torr produces both neutral atomic Al (I) and singly charged Al (II) ions, as also seen in other work [18]. High-resolution spectra were measured with a 2400 gr/mm grating. Atomic Al (I) with characteristic doublet peaks at 394.4 nm and 396.1 nm, and singly charged Al (II) with a peak at 466.3 nm [19] are shown below in Fig. 5a. The ratio of ions to neutrals is a function of laser fluence and this ratio increases with increasing fluence. Below 6 J/cm^2, Al ions were too low in intensity to be detected.

When air is introduced into the chamber, there is a dramatic visual change in the color of the ablation plume. It changes from a pale violet to a turquoise. In the presence of air at pressures of 0.5 Torr and greater, atomic and singly ionized Al are still readily detected, even at delays < 1μs, however, distinct vibrational bands from molecular AlO are observed after a 10-μs delay [20]. AlO vibrational bands at 2 Torr air are shown in Fig. 5b. The vibrational transitions are from levels in the $B^2\Sigma$ - $X\ ^2\Sigma$ electronic transition [21] with a series of vibrational band sequences (Δv = 3, 2, 1, 0, -1). These AlO bands are absent in the high-vacuum ablation plume.

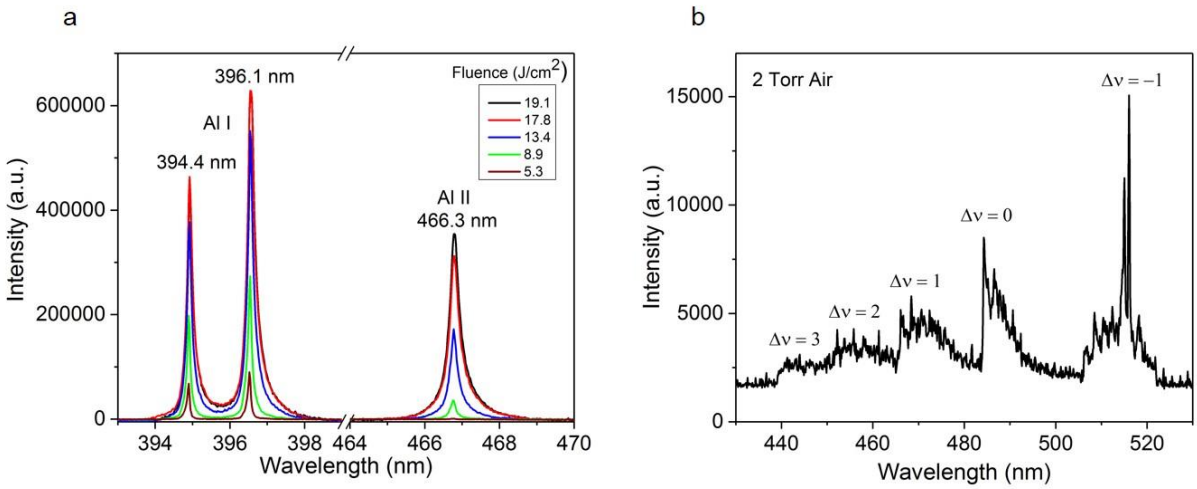

Fig. 5. (a) Emission from atomic (Al I) and singly ionized (Al II) aluminum as a function of incident laser fluence. (b) Molecular emission spectra from vibrational bands in AlO measured in the laser ablation plume in 2 Torr of air

Emission from atomic Al (Al I) at 394.4 nm and 396.1 nm are measured as a function of distance from the target (2 - 6 mm) and time delay (0 – 1000 ns). This allows a calculation of the velocity of aluminum atoms. The propagation of the ablated plume of aluminum atoms can be monitored by measuring emission intensity as a function of time (Fig. 6). From these measurements, the axial front velocity of the Al atoms can be calculated, which is on the order of 20 km/s

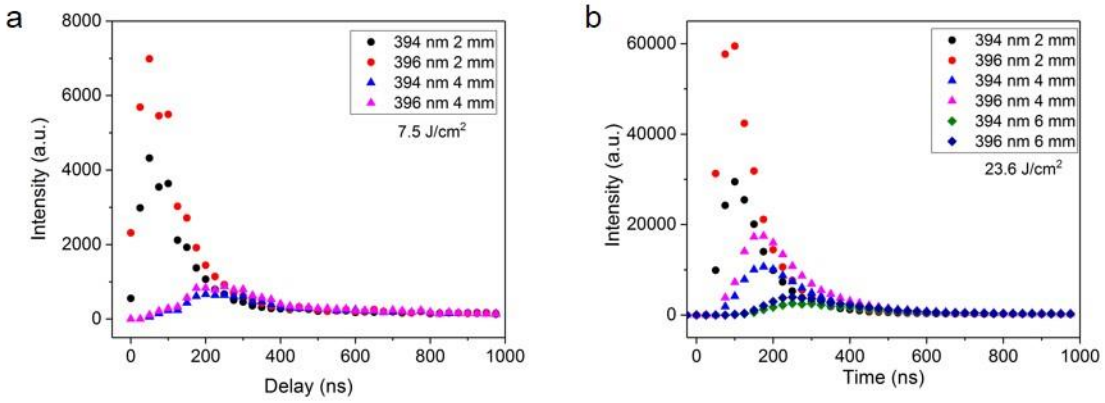

Fig. 6. Time-resolved measurement of atomic Al I emission at varying distances from the target surface, measured at laser fluences of (a) 7.5 J/cm^2 and (b) 23.6 J/cm^2. The emission intensities increase with increasing laser fluence.

Plume spectra measured during the hypervelocity impact on DebriSat [16] showed a complex set of spectral lines that stemmed from various materials comprising the components inside the satellite structure. Atomic emission lines from Al, Fe, and Cr were seen, and in addition, molecular bands from AlO and C_2 were observed [16]. There was also a notable absence of ions in the spectra, and while Al (II) was a possible candidate, it was not dominant.

Optical reflectance measurements were made on the ablation deposits collected on polished copper and fused silica substrates. The uncoated Cu substrates are reflective, but as they were not polished to an optically smooth finish, they show a small, but measureable diffuse component.

Significant differences can be observed in the optical reflectance measured on ablated deposits on Cu substrates, produced in high-vacuum and in air, with ablations conducted at 7 J/cm^2 (Fig. 7). A reflective Al film is deposited in high-vacuum. The total hemispherical reflectance (Fig. 7a) of the deposited Al film (blue curve) is lower than that of the uncoated Cu substrate and is also lower than the simulated reflectance of a pure Al film (green curve), from a fit using optical constants for Al [21]. This loss could be attributed, in part, to scatter from splats as described earlier [15].

In contrast, as discussed earlier, ablation of 6061 Al in 2 Torr of air produces aluminum oxide filaments and aluminum oxide-covered Al particles. Although the exact stoichiometry of this oxide deposit has not been established, it is transparent in the UV-visible spectral range, producing an optical reflectance curve that closely tracks that of the Cu substrate. The diffuse reflectance due to this deposit is measurably higher than that of the Cu substrate, and increases as the wavelength decreases from 2500 nm down to 600 nm. This behavior could be due to scatter from Al_xO_y -covered Al particles that get co-deposited with the filamentous material. There may also be some absorption from the porous matrix of Al_xO_y filaments.

Below 500 nm, the absorption edge of Cu limits the measurement, and this complicates the interpretation of the diffuse reflectance at shorter wavelengths. Hence we deposited materials on fused silica substrates that are completely transparent in the wavelength region 200-2500 nm, thus without interference from an absorption edge. This makes the differences between laser ablated deposits from 6061 Al in high vacuum and in air, and Al-composite are even more striking.

In total reflectance (Fig. 7b), the reference uncoated fused silica substrate has a very low reflectance (< 4%). The Al_xO_y film, deposited in 2 Torr air has a similar low reflectance as the fused silica substrate, while the metallic Al film deposited in high-vacuum is highly reflective (60-80%). The deposit from the Al-composite, laser-ablated in high-vacuum, is ~ 20-40% reflective at wavelengths > 1500 nm, but drops to 15-20% at wavelengths < 1000 nm.

In transmission (Fig. 7c), fused silica is 90% transmitting over the entire wavelength range. Al_xO_y is also nearly 90% transparent, while Al has a transmission of < 5%. The laser ablated deposit from the Al-composite is ~ 60% transmissive between 1500 – 2000 nm, but its transmission drops to 0% < 500 nm. In high-vacuum, the Al-composite target appeared to selectively ablate the composite, and not the Al.

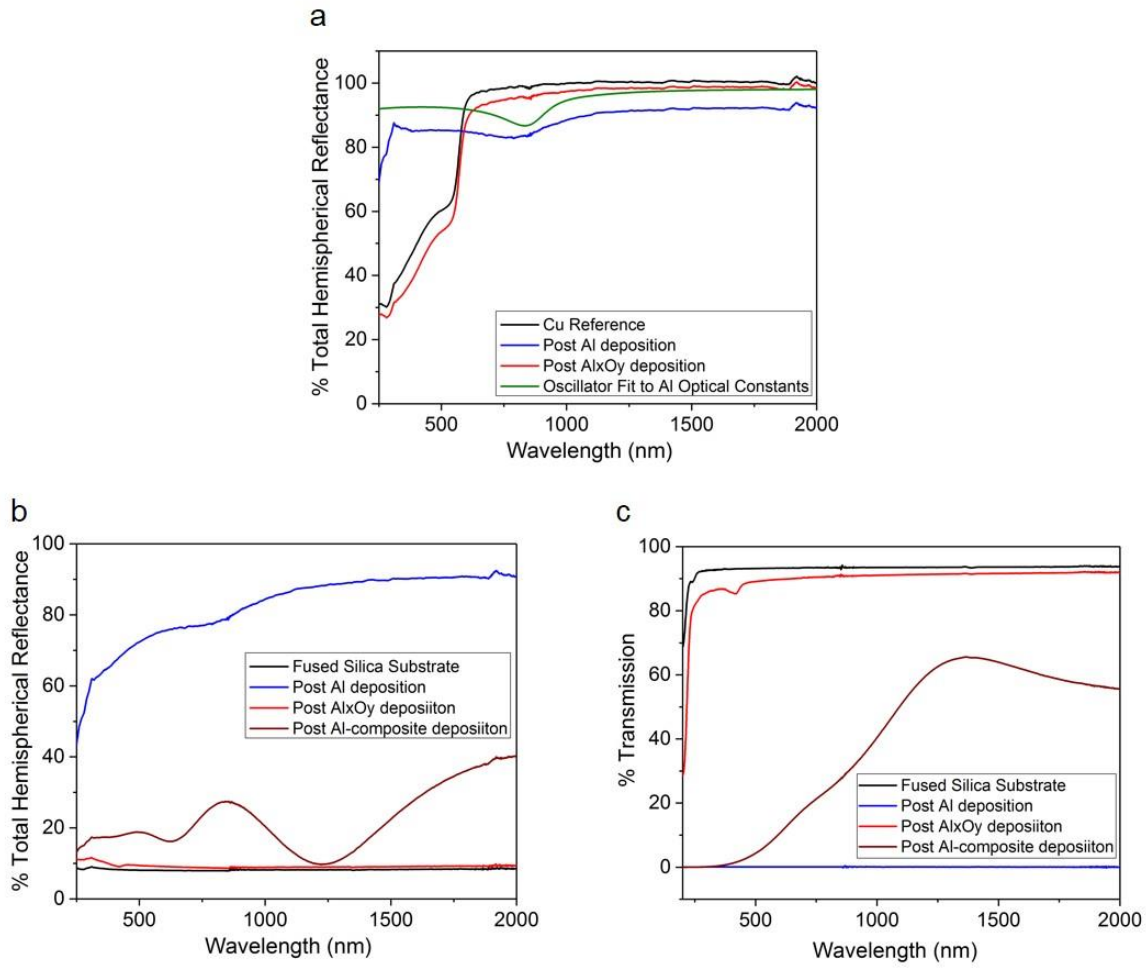

Fig. 7. (a) Cu substrate: Total Hemispherical Reflectance - uncoated Cu substrate (reference) and laser ablated Al in air (forming Al_xO_y) and in high-vacuum (metallic Al); also shown is an oscillator fit to pure Al film derived from optical constants; (b) Fused silica substrate: Total Hemispherical Reflectance - uncoated fused silica substrate (reference) and laser ablated Al in air (forming Al_xO_y) and in high-vacuum (metallic Al), and Al-composite in high-vacuum; (c) Fused silica substrate: Transmission - uncoated fused silica substrate (reference) and laser ablated Al in air and high-vacuum, and laser ablated Al-composite in high-vacuum.

The key point we would like to emphasize is that the optical behavior of Al metal which is produced in 10^{-8} Torr vacuum is very different from that of filamentous AlxOy that is generated from impact to a metallic Al target in air. In addition, the optical properties of the deposits from the Al-composite ablated in high-vacuum, are quite different from those of metallic Al also produced in high-vacuum. Hence these differences are relevant to albedo interpretations leading to physical size measurement. The observed differences are due to the chemical differences in materials that are produced from impacts in different environments, in high-vacuum (as in LEO) versus air (as in HVI on ground), thus resulting in different optical properties.

Specular reflectance from DebriSat witness coupons is shown in Fig. 8. The reflectance was reduced to almost 0%, and we attribute this to condensed vaporized foam and disordered graphitic carbon from the catch panels that covered the satellite material debris [14]. The presence of foam was confirmed by its signature in Fourier Transform Infrared spectroscopy [21]. As the same was observed with DebrisLV, which had no composite facesheet, we are confident that the composite facesheet was not contributing to the darkening. Due to the intense foam coverage, the true albedo of the collected debris could not be measured.

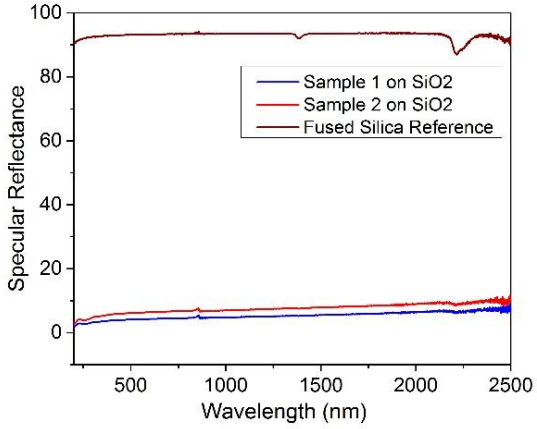

Fig.8. Optical reflectance measured on coupons from DebriSat field experiment

4. CONCLUSIONS

Excimer laser ablation of a 6061 Al target at 248 nm was used to simulate hypervelocity impact experiments. Experiments were conducted in 2 Torr of air to replicate results from the DebriSat test of 2014. The morphology of debris collected at 2 Torr is similar to that of material collected from the DebriSat hypervelocity impact. In high-vacuum (of 10^{-8} Torr), the results are very different. An Al film and Al particles are created, and the optical reflectance is that of a lossy Al film. The loss is primarily due to scatter from particles. In air, the Al film is replaced by Al_xO_y filaments and Al particles that are covered by a sheath of fuzzy Al_xO_y. This leads to a very different optical reflectance spectrum, with the transparent Al_xO_y tracking the substrate reflectance, coupled with scattering losses due to the Al particles present in Al_xO_y filaments and possibly absorption losses from the porous matrix at shorter wavelengths in the UV. An Al-carbon-fiber reinforced composite target was also ablated in high vacuum and showed optical signatures that were different from both Al and Al_xO_y. These results and the measured differences between air and high-vacuum have relevant implications for the determination of physical sizes of orbital debris in LEO or GEO that are based upon optical measurements that use albedo as a critical parameter.

5. ACKNOWLEDGEMENTS

We gratefully acknowledge Vale Sather, Sam Peresztegy, Anthony Salvaggio, Sumner Matsunaga, and Tom Huynh for their support of this work. Financial support was provided from AF SMC. We would like to thank Peter Fuqua, James Barrie, Heinrich Muller, Marlon Sorge, and Heather Cowardin for valuable discussions.

6. REFERENCES

1. D. Hampf, P. Wagner, W. Riede, Optical Technologies for Observation of Low Earth Orbit Objects, 65th Int. Astronautical Congress, Toronto, Canada, IAC-14 A6.P, 1-8, 2014 .
2. J.R. Shell, Optimizing Orbital Debris Monitoring with Optical Telescopes, AMOS 2002.
3. D. Hampf, W. Riede, G. Stockle, I. Buske, Ground-Based Optical Position Measurements of Space Debris in Low-Earth Orbits, Deutscher Luft- und Raumfahrtkongress, 301313 1-10, 2013.
4. M. Mulrooney and M. Matney, Derivation and Application of a Global Albedo Yielding an Optical Brightness to Physical Size Transformation Free of Systematic Errors, Proc. 2007 AMOS Conference, HI, 709-728, 2007.
5. M. Mulrooney, M. Matney, and E. Barker, A New Bond Albedo for Performing Orbital Debris Brightness to Size Transformations, 2008 Int. Astronautical Congress, Glasgow, Scotland.
6. A.E. Potter, K.G. Henize, and D.L. Talent in *Orbital Debris from Upper-stage Breakup*, Ed. J.P. Loftus, A90-18004 05-12, Washington, DC, AIAA 147-156, 1989.

7. H. Cowardin, K. Abernathy, E. Barker, P. Seitzer, M. Mulrooney, T. Schildknecht, An Assessment of GEO Orbital Debris Photometric Properties Derived from Laboratory-Based Measurements, *https://ntrs.nasa.gov/archive/nasa/casi.ntrs.nasa.gov/2009*.
8. Syuzo Isobe et al., A new 1 m telescope for space debris survey observations, Advances in Space Research, 34, 917 920, 2004.
9. K. Jorgensen, J. Africao, K. Hamada, E. Stansbury, P. Sydney, P. Kervin, Physical Properties of Orbital Debris from Spectroscopic Measurements, Advances in Space Research 34, 1021-1025, 2004.
10. D.J. Kessler, K.S. Jarvis, Obtaining the Propertly Weighted Average Albedo of Orbital Debris from Optical and Radar Data, Advances in Space Research 34, 1006-1012 2004.
11. A. N. Pirri, Theory for Laser Simulation of Hypervelocity Impact, Physics of Fluids, 20 221-228, 1977.
12. B. Arad, S. Eliezer, I. Gilath, E. Moshe, C.G. Simon, Laser Simulation of Hypervelocity Impacts in Space, Trans. on the Built Environment, 19, 431-440, 1996.
13. J.D. Tandy, J.M. Mihaly, M.A. Adams, and A.J. Rosakis, Examining the Temporal Evolution of Hypervelocity Impact Phenomena via High-speed Imaging and Ultraviolet-visible Emission Spectroscopy, Journal of Applied Physics 116, 034901 1-13, 2014.
14. D. Heunoske, M. Schimmerhorn, J. Osterholz, and F. Schäfer, Time Resolved Emission Spectroscopy of Impact Plasma, Procedia Eng. 58 2013 624-633.
15. G. Radhakrishnan, P.M. Adams, C.J. Panetta, and Diana R. Alaan, Comparison of Laser Ablation Effects to Hypervelocity Impact and Debris Darkening, paper presented at the 14th Hypervelocity Impact Symposium 2017, HVIS2017, 24-28 April 2017, Canterbury, Kent, UK; in press, Procedia Engineering, July 2017.
16. G. Radhakrishnan, Time-resolved spectroscopy of plasma flash from hypervelocity impact on DebriSat, The 13th Hypervelocity Impact Symposium, Procedia Eng. 103 507-514, 2015.
17. P.M. Adams, P. Sheaffer, Z. Langley, G. Radhakrishnan, Characterization of Hypervelocity Impact Debris from the DebriSat Tests, AMOS 2017 Conference, to be published.
18. J. T. Knudtson, W. B. Green, and D.G. Suttton, The UV-visible spectroscopy of laser-produced aluminum plasmas, J. Appl. Phys. 61 4771-4780, 1987.
19. NIST Atomic Spectra Database, http://physics.nist.gov
20. S.S. Harilal, B.E. Brumfield, Bret D. Cannon, and Mark C. Phillips, Shock Wave Mediated Plume Chemistry for Molecular Formation in Laser Ablation Plasmas, Anal. Chem. 88, 2296-2302, 2016.
21. R.W.B. Pearse and A.G. Gaydon, *The Identification of Molecular Spectra*, 3rd Ed., Chapman and Hall Ltd. London, 1965.
22. E.D. Palik, *Handbook of Optical Constants of Solids II*, Elsevier Science (USA) 1998.